ISSN 0031-918X, The Physics of Metals and Metallography, 2015, Vol. 116, No. 5, pp. 456–466. © Pleiades Publishing, Ltd., 2015.
Original Russian Text © V.A. Beloshenko, V.Yu. Dmitrenko, V.V. Chishko, 2015, published in Fizika Metallov i Metallovedenie, 2015, Vol. 116, No. 5, pp. 484–495.

STRUCTURE, PHASE TRANSFORMATIONS, AND DIFFUSION

Modifying the Structure and Properties of Cu–Fe Composites by the Methods of Pressure Formation

V. A. Beloshenko, V. Yu. Dmitrenko, and V. V. Chishko

Galkin Donetsk Institute for Physics and Technology (DonPT), National Academy of Sciences of Ukraine, ul R. Luksemburg 72, Donetsk, 83114 Ukraine

e-mail: dmitrenko_v@mail.ru

Received June 14, 2014; in final form, November 12, 2014

Abstract—In this survey, the results of the available studies are generalized and the effects of thermomechanical treatment on the structure and the magnetic, mechanical, and electrical properties of Cu–Fe composites produced by the methods of casting, powder metallurgy, and severe plastic deformation are analyzed. The primary attention is paid to the method of packet hydroextrusion, which makes it possible to achieve a wide spectrum of diameters (3 nm–2 mm) of iron fibers and of the amount of fibers ($1–8 \times 10^8$) in these composites with varying volume content (10–60%). The physical mechanisms of the revealed effects of the structural modification of the physicomechanical characteristics on different scale (macro, micro, and nano) levels are discussed.

Keywords: Cu–Fe composites, plastic deformation, nanostructure, mechanical properties, electrical conductivity

DOI: 10.1134/S0031918X1505004X

1. INTRODUCTION

Copper-based binary systems with limited solubility (Cu–Nb, Cu–Fe, Cu–Cr, Cu–Ag, etc.), in which no intermetallic compounds are formed, belong to a class of materials that combine high strength and high electrical conductivity [1]. The priority fields of their use include instrument making (pulsed high-field magnets, magnetic drives) [2, 3], power engineering (electric-power lines, the contact elements of power lines of electric transport) [2, 4], microelectronics, spintronics, etc. [5].

The wide spectrum of the application of Cu–Fe composites is due to their unique complex of physicomechanical properties, e.g., excellent thermal and electrical conductivity, good mechanical properties, and high wear and corrosion resistance, in combination with the good manufacturability and the low cost of iron compared with other possible materials (Nb, Cr, Ag, Au). The most important task in the field of creating composites of this class is the development of methods of the directional regulation of their structure and properties, which would ensure the required operating characteristics. In this survey, we present the results of studies that concern the influence of the method of preparation and thermomechanical processing on different properties of nanostructured Cu–Fe composites. We consider the changes in the physicomechanical characteristics of these materials at different scales and (macro, micro, and nano) structure levels in the course of severe plastic deformation (SPD) with the use of packet hydroextrusion in great detail.

2. TRADITIONAL METHODS OF FABRICATING Cu–Fe COMPOSITES

When constructing composites, in addition to appropriately selecting the material of the components and the geometry of their arrangement, which determine the opportunity of achieving the required complex of properties, the correct selection of the most efficient and economical technology of their production is also of exceptional importance. At present, several thousand methods of obtaining composite materials are known [6]. The expediency of applying a given technological process is determined by the specific features of the materials of composites, the requirements to their surface quality, and the accuracy of sizes, as well as based on the technical, economical, ecological, and other indices. In the overwhelming majority of cases, the composite material is not subjected to mechanical treatment after preparation, since this can lead to the loss of a many or all of its advantages. Therefore, as a rule, technologies oriented toward the production of specific types of articles have been developed. The traditional methods of obtaining Cu–Fe composites include liquid-phase methods, gas-, and vapor-phase methods, and chemical methods that use powder metallurgy.

2.1. Liquid-Phase Methods

Liquid-phase methods (casting, directional crystallization) make it possible to use the nondeformable casting alloys as a matrix and to produce articles of complex configuration without additional formation. At the same time, these methods make it possible to obtain layered ingots with round cross sections suitable for further working under pressure (by rolling, extrusion, drawing). The authors of [7, 8] have investigated the structure and properties of a Cu–Fe composite obtained by casting with subsequent drawing. After casting, the structure of the composite is characterized by the presence of large dendrites of iron with a certain amount of dispersed particles of iron. Upon deformation by drawing, iron dendrites become elongated in the direction of drawing up to the formation of nanodimensional fibers [7–9]. The cross sections of dendrites have a filamentary morphology that results from the joint deformation of copper and iron, which is characteristic of fcc fibers in a bcc matrix [10]. X-ray diffraction analysis has shown that the fibrous structure formed in the process of drawing is characterized by preferred crystallographic orientations of the Cu ⟨110⟩ and Fe ⟨100⟩ types in the longitudinal section and Cu ⟨111⟩ and Fe ⟨110⟩ types in the transverse section [7]. The formation of a similar structure in the Cu–Fe composite was also observed in the case of deformation by cold rolling [1].

As a result of the formation of a fibrous structure and the related reduction in the mobility of dislocations blocked by the branched interphase boundaries [2], the Cu–Fe composite acquires higher mechanical properties compared with those predicted by the rule of mixtures [8, 9, 11]. In this case, the hardness and ultimate strength correlate with the sizes of the iron fibers and with the spacings between them, (which change nonmonotonically with an increase in the stored deformation) rather than with the degree of strain [7–9].

The Cu–Fe composites represent the greatest interest from the viewpoint of the combination of high strength and low electrical resistance. The relationship between these parameters can be controlled by (1) changing the volume content of Fe, (2) alloying, and (3) thermomechanical treatment. It has been shown in [4] that, with an increase in the iron content from 10 to 30 wt %, the ultimate strength of the Cu–Fe composites obtained by casting increases from 950 to 1310 MPa, and the electrical conductivity decreases from 69 to 55% IACS. The authors of [12–16] have investigated the influence of the alloying by Ag, Zr, and by rare-earth elements (REs) on the structure and physicomechanical properties of cast Cu–Fe composites. The addition of these elements can lead to a twofold decrease in the size of the primary iron dendrites and copper grains in the cast sample, which, upon subsequent cold deformation, leads to a 50% increase in the ultimate strength with an insignificant reduction in the electrical conductivity compared with the unalloyed composite. A substantial increase in the electrical conductivity (to 40%) with a minimum loss of the strength (~10%) can be achieved using intermediate heat treatments (HTs) in the technological process, which lead to a decrease in the number of centers of the scattering of charge carriers in the copper matrix due to the precipitation of impurities and alloying elements [16].

The thermomechanical treatment plays a decisive role in the optimization of the strength–electrical-conductivity ratio of Cu–Fe composites. It should be noted that the Cu–Fe alloys have a lower conductivity compared with other composites with the copper matrix (Cu–Ag, Cu–Nb, Cu–Ta, and others). The reason for this lies in the relatively high solubility of iron in copper at high temperatures in combination with the slow kinetics of its precipitation at lower temperatures, as well as in the negative effect of the Fe atoms present in the solid-solution state on the conductivity [4, 12]. Thus, upon the thermomechanical treatment of Cu–Fe composites, it is important to minimize the formation of the solid solution of iron in copper.

2.2. Chemical and Gas- and Vapor-Phase Methods

Chemical and gas- and vapor-phase methods of fabricating composites are most efficient in the production of multilayer films and the application of thin coatings. The advantages of these methods include the absence of softening and significant mechanical stresses of the reinforcing elements and the matrix, avoiding direct contact between the reinforcing elements, and the opportunity for articles and semifinished products of complex configurations to form. The shortages of these methods lie in the difficulty of using complex-alloy materials as the matrices, as well as the possibility of crack formation and stratification under the conditions of a complex stressed state. The application of methods of this group for obtaining Cu–Fe composites makes it possible for effects connected with the low dimensionality of the system (thickness of the layers can be varied from 5 to 50 Å) to appear, such as superplasticity [17], the absence of the interdiffusion of copper and iron [17], and negative magnetoresistance [18]. The observed strong dependences of the magnetic and conducting properties on the number and thickness of layers of Cu and Fe [5, 19–21] and the opportunity to precisely control these parameters, which are ensured by the production method, open wide prospects for applying multilayer Cu–Fe laminates in microelectronics and spintronics [5].

2.3. Powder-Metallurgy Methods

The advantages of the powder-metallurgy methods consist of the opportunity of using hard-to-deform metals, alloys, and compounds as matrices; achieving

high concentrations of the reinforcing phase (more than those maximally possible upon the packaging); the combination of reinforcement with precipitation strengthening; and the use of standard equipment. The drawbacks of these methods include the nonuniformity of the distribution of short fibers over the volume of an article due to nodulization in the course of mixing the charge with the fibers; the opportunity of a damaging of brittle fibers upon the mixing, compacting, or deformation of multifibrous composite materials; the increased content of oxides and other impurities because of the developed surface area of matrix powders; and porosity (depending on the method utilized).

The structure and physicomechanical properties of Cu–Fe composites obtained by the methods of powder metallurgy have been investigated in [10, 22–27]. The evolution of the structure was similar to that observed in the case of cast composites; upon drawing, the iron particles assume a fiberlike morphology in the longitudinal section and a filamentary morphology in the transverse section [10, 22–24]. In contrast to the cast samples, coarse particles are present, which represent complex oxides of iron and copper and remain undeformed, even after high degrees of drawing [22].

As in the case of cast samples, the strength (and partly the conductivity) of the Cu–Fe composites obtained by the methods of powder metallurgy is determine by the size and spatial distribution of the iron fibers and, to a certain extent, by the mechanical properties of the initial components, such as their elasticity moduli [24]. It has been shown in [23] that the ultimate strength of the Cu–20 wt % Fe composite exceeds that of Cu–20 wt % Nb after the identical degree of deformation and correlates with the larger value of the shear modulus of Fe compared with that of Nb. The strength of Cu–Fe composites also increases with a decrease in the initial size of iron powder particles [23]. The key factor in obtaining high conductivity of the system in question is the control of conditions of consolidation (time, temperature) for decreasing the dissolution of Fe in Cu. Thus, it has been established in [24] that, at a consolidation temperature of less than 525°C, a decrease occurs in the conductivity of the Cu–Fe of composites by less than 1% IACS. This allowed the authors of [24] to exceed the best commercial alloys in terms of the strength/conductivity ratio and to compete with systems like Cu–Nb, Cu–Ta, and Cu–Cr. The use of reduced consolidation temperatures (<500°C) favors the formation of a composite structure with nanosized grains of Cu and Fe [26].

The data concerning the magnetic properties of the alloys in question are quite scarce. The magnetic parameters of Cu–Fe composites (Curie temperature, coercive force, saturation magnetization) obtained by the methods of powder metallurgy have been analyzed in [25, 27]. It has been shown that the dependence of the coercive force H_c on the time of milling (t = 1–72 h) of the initial powders in a ball mill is nonmonotonic with a maximum $H_c \approx 140$ Oe at $t = 30$ h and minimum $H_c < 5$ Oe at $t = 72$ h [27]. In this case, the size of the grains of copper and iron decreases monotonically (to 18 nm) as t increases to 30–40 h, after which it stabilizes on the level of 20 nm. This $H_c(d)$ dependence contradicts the known data [28], according to which the coercive force monotonically increases with a decrease in the size of iron grains up to a certain critical value (6–25 nm, according to different authors), after which there occurs a transition into a superparamagnetic state. The authors of [27] do not explain the discovered effect. At the same time, with an increase in milling time, a substantial increase is observed in the lattice parameters of Cu and Fe, which indicates the formation of the solid solution of iron in copper [27]. According to the data of [29], this may be the reason for the observed effect.

The application of powder-metallurgy methods for obtaining Cu–Fe composites using low temperatures of consolidation causes a lowered content of the solid solution of Fe in Cu compared with the liquid-phase methods and, correspondingly, an increased electrical conductivity with the retention of the strength properties.

3. APPLICATION OF METHODS OF SEVERE PLASTIC DEFORMATION IN THE TREATMENT OF Cu–Fe COMPOSITES

It is known that the nanostructured composites, in which the content of one of the components varies from a few fractions of a percent to several tens percent, and the sizes vary in the range of 10–100 nm, possess extremely high catalytic, magnetic, and tribotechnical characteristics, as well as high thermal and chemical stability, high strength, high plasticity, etc. The components of the composite materials obtained using the traditional methods of pressure forming (extrusion, rolling, drawing) usually have micron or submicron sizes [30]. The production of nanostructures by the aforementioned methods is by no means always justified, since in these cases, the transverse dimensions of the samples multiply decrease, which limits the field in which they are subsequently used. Methods of the plastic deformation in which the dimensions of the sample either do not change or periodically return to the initial dimensions nullify the noted disadvantages and create an opportunity to repeatedly treat the sample with the accumulation of large deformation. This leads to the appearance of a nanostructure, which in turn provides a substantial improvement in the properties of the material. These methods include SPD techniques, such as high pressure torsion (HPT), all-round rotary forging, screw extrusion, equal-channel angular pressing, accumulative roll bonding (ARB), and packet hydroextrusion (PHE) [31–33]. According to the available literature data, the application of SPD in the

case of Cu–Fe composites includes HPT, ARB, and PHE.

3.1. High-Pressure Torsion

During HPT, the sample mainly undergoes shear deformation. In [31, 34], the HPT was used to form a nanocrystalline structure in a fiber-like Cu–Fe composite obtained by cold drawing. Along with a decrease in the size of grains (to below 50 nm), the disappearance of fibers, the homogenization of the structure, and the significant (to 85%) dissolution of iron in copper were observed. It has been established that, with an increase in the degree of deformation (with grain refinement), a transition occurs from the ferromagnetic to superparamagnetic state [29]. The authors of [29] have not presented the dependence of the magnetic properties of the composite on the degree of deformation and/or on the size of structural elements. They also have not investigated the thermal stability of the nanostructure that arises, which may prove to be considerably lower than that in the initial composite. The application of this method is limited because of the small dimensions of the samples employed.

3.2. Accumulative Roll Bonding

The essence of this variant of the SPD method consists in assembling a packet of alternating sheets and subsequently rolling the packet to a thickness equal to the that of a single initial layer that makes up the composite. Then, the obtained rolled sheet is cut, the next packet is assembled, and this technological cycle is repeated until the required thickness of the layers is obtained in the sample [35]. Thus, several passes are performed, the number of which is limited by the dimensions of the sample, which decrease as the edges are cut. The authors of [36–40] have investigated the opportunity of obtaining bulk Cu–Fe nanolaminates using a method based on multiple repetitions of a technological cycle that includes vacuum hot rolling and subsequent rolling in air. With an increase in the number of passes, a fourfold decrease is observed in the number of layers of Cu and Fe in the composite connected with the mutual solubility of copper and iron, which leads to an increase in their sizes [39–41]. The second problem consists in the presence of regions of the local collapse of copper layers, which is negatively reflected on the properties of the Cu–Fe composite [36, 42]. The yield stress, the ultimate strength σ_u, and the hardness of these composites grow with an increase in the number of layers, which is caused by the manifestation of nanostructure effects [36, 38]. Data on the resistive properties of bulk multilayer Cu–Fe composites are absent.

3.3. Packet Hydroextrusion

The packet HE consists in multiple repetitions of the operations of assembling composite samples, which consist of a tubular shell with a packet of rodlike elements, the hermetic sealing of these packets, and evacuation with subsequent deformation by HE [43]. The use of high hydrostatic pressure ensures the reliable cohesion of the elements of the composite samples without an additional thermal action, their proportional extrusion in the course of their joint plastic deformation, and the realization of an ultrahigh accumulated deformation [44, 45]. In this case, in view of the hydrostatic character of the deformation conditions, a hexagonal close packing of the component elements is automatically achieved in the packet with the formation of high-angle boundaries between them [44]. Thus, this method can be successfully used to produce nanocomposites.

In [46], the method of PHE in combination with drawing has been used to obtain fibrous Cu–Fe composites with the number of fibers of up to 19×7^7 pieces. It has been discovered that, with a decrease in the diameter of fibers to 10 nm, the coercive force increases monotonically. This contradicts the results of [47–49], where it has been shown that ferromagnetism disappears at sizes of iron particles of approximately 6–10 nm. This contradiction can be explained by the discrepancy between the calculated and true diameters of the iron fibers [46]. The studies by the method of transmission electron microscopy have shown that the true diameter of the iron fibers in the Cu–Fe composites in the nanodimensional region is five to seven times greater than the calculated diameter [46]. Consequently, the authors of [46] did not achieve the maximum value of the coercive force which is observed at a certain critical dimension of iron particles [48]. A number of problems remained unexplained with regard to the influence of deformation on the magnetic susceptibility, Curie temperature, and the mechanical and resistive properties of the Cu–Fe composites.

These problems are considered in [50–54]. The structures of the aforementioned composites made it possible to obtain a wide spectrum of diameters and numbers of fibers (n_f) in the wire samples by varying their volume content (table). This made it possible to establish the influence of the structural modifications upon SPD on the complex of physicomechanical properties upon the transition from macro- to micro- to nanosized fibers.

3.3.1. Structure of the composites. The X-ray diffraction analysis of the Cu–Fe composites has shown that they represent a two-phase system with a component ratio close to the calculated value. The experimental and computed values of the volume fraction of iron in the composite are equal to 56 and 58% for $n_f = 1$, 41 and 39% for $n_f = 211$, 30 and 27% for $n_f = 211^2$, 22 and 18% for $n_f = 211^3$, and 12 and 13% for $n_f =$

Characteristics of Cu–Fe composites

Diameter of the sample D, mm	Number of fibers n_f	Diameter of fibers d_f, μm	Coefficient of the volume content of iron K
3	1	2280	0.58
	211	130	0.39
	211^2	7.4	0.27
	211^3	0.42	0.18
	85×211^3	0.038	0.13
0.21	1	160	0.58
	211	9	0.39
	211^2	0.52	0.27
	211^3	0.029	0.18
	85×211^3	0.003	0.13

85×211^3. The diffraction pattern of the deformed composite demonstrates the presence of a strong crystallographic orientation as follows: the (200) reflection of iron characteristic of the misoriented crystals is absent; the (211) and (220) reflections of iron and the (220), (222), and (311) reflections of copper are weakly pronounced; and the intensity of the reflection (110) of iron is large (Figs. 1a, 1b). This texture is characteristic of the iron and steel wires obtained by drawing [55]. In the copper matrix, a texture with a preferred direction (111) also arises.

Passage into the region of nanodimensional fibers is characterized by a decrease in the intensity of lines and by growth in the background in the diffractograms. At the diameter of the fibers $d_f = 3$ nm, the (110) line of the bcc iron (Fig. 1c) disappears, which can be connected with the breakdown of fibers into fragments and the formation of a solid solution of iron in copper [34, 56, 57]. The last assertion is also confirmed by the behavior of the lattice parameters of iron and copper, which grow with a decrease in the diameter of fibers. The lattice parameters can also increase due to an increase in the amount of crystal-structure defects. The sizes of the coherent domains decrease monotonically to 20 nm with a decrease in the diameter of fibers, which indicates the formation of a nanocrystalline structure in the samples under investigation (Fig. 2).

3.3.2. Mechanical properties. The dependences of the ultimate strength σ_u on the volume fraction of iron K and the fiber diameter d_f are nonmonotonic (Fig. 3) [51, 52]. With decreasing K and d_f, three characteristic regions can be separated: region of $d_f \geq 10$ μm, in which σ_u decreases significantly; $d_f \sim 30$–9 μm, where the ultimate strength grows; and $d_f < 30$ nm, in which again there is observed a softening of the composite. In the range of $d_f < 10$ μm, the dependences obtained are described well by the rule of mixtures under the condition of equal deformations. With decreasing d_f ($K \leq 0.4$), the rule of mixtures is violated and the ultimate strength of the composites grows substantially. It can be assumed that the observed deviation from the rule of mixtures is caused by the action of the mechanisms of strengthening of the composites related to the generation and movement of dislocations. After a certain critical dimension is reached ($d_f \sim 30$ nm), a transition is observed from the processes described by the Hall–Petch relation (influence of grain boundaries on the multiplication and movement of dislocations) to the processes connected with the dislocation slip along grain boundaries [58]. In this case, processes of dynamic recrystallization in the copper matrix can occur. As a result, the ultimate strength decreases.

The dependences of the relative elongation and Vickers hardness H_V of the fibrous Cu–Fe composites on K and d_f are qualitatively similar to those characteristic of the ultimate strength [51]. At the same time, the increase in H_V upon the transition into the submicron region of d_f is noticeably less than that for σ_u. This is explained by the following. The value of H_V at $d_f \approx 160$ μm (bimetal) is mainly determined by the hardness of iron. At smaller sizes of fibers (at other standard sizes of the composite components), the size of the imprint of the indenter significantly exceeds d_f, and H_V is already a certain integral quantity determined by the iron fibers and copper matrix. Therefore, an increase in H_V with the decrease in d_f is relatively small due to an increase in the contribution from the softer copper component of the composite. Heat treatment leads to a decrease in the values of σ_u and H_V without a change in the character of the dependences described in [51].

3.3.3. Magnetic susceptibility and magnetization. The decrease in the size of the fibers of the deformed samples leads to a reduction in the magnetic susceptibility and saturation magnetization and to an increase in the remanence. A transition is observed from the soft-magnetic to the hard-magnetic state. The hysteresis loops of the magnetic susceptibility have an ordinary character: at the strength of the magnetic field

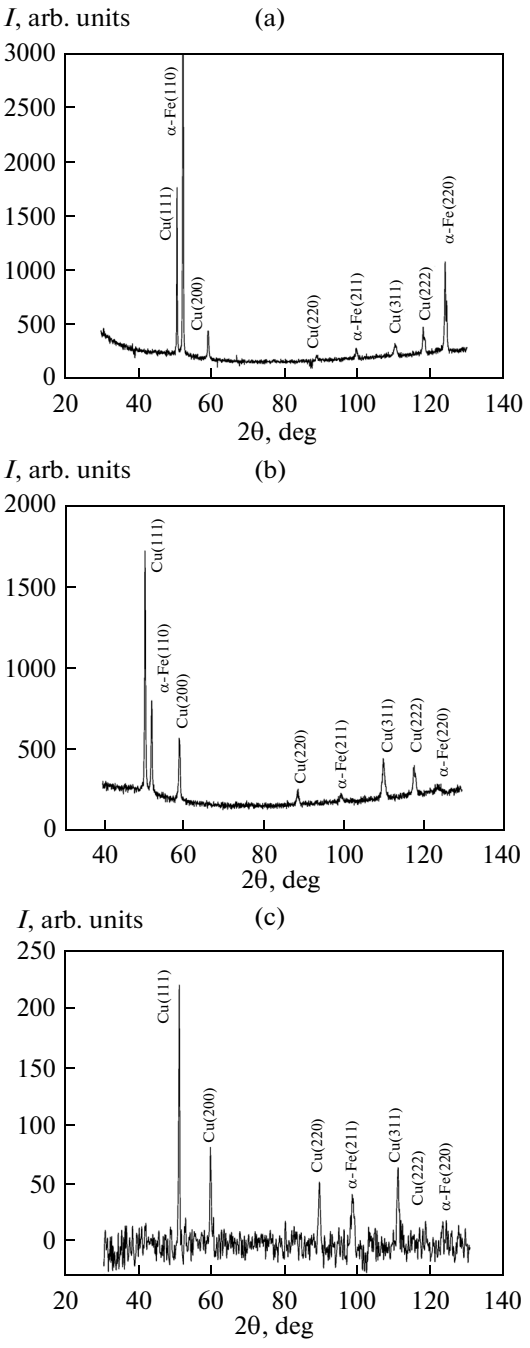

Fig. 1. X-ray diffraction patterns of Cu–Fe composites with different diameters of the fibers d_f: (a) 2.88 mm, (b) 130 μm, and (c) 3 nm.

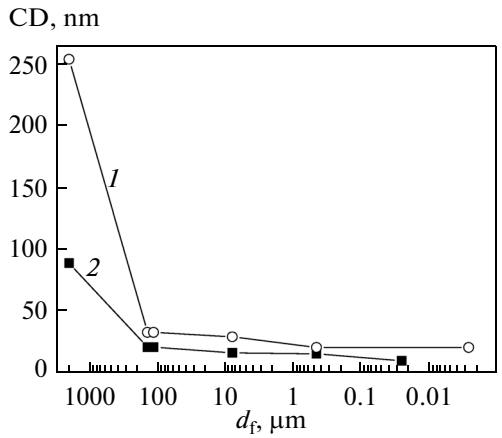

Fig. 2. Size of coherent domains (CD) in (*1*) the copper and (*2*) iron components of Cu–Fe composites as a function of the diameter of the iron fibers.

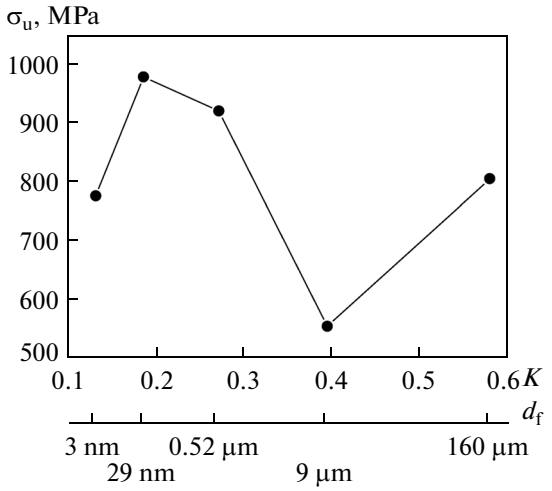

Fig. 3. Dependence of the ultimate strength σ_u of Cu–Fe composites on the volume content of iron and diameter of iron fibers.

$H > 0$, the ascending branches of the hysteresis loops lie above the descending branches, and vice versa at $H < 0$ [50].

The heat treatment of samples at $T = 550$°C increases the magnetic susceptibility. At a fiber size of $d_f = 130$ μm, anomalies are observed in the behavior of the hysteresis loops. At $H \approx \pm 130$ Oe, the ascending and descending branches intersect and change places (the hysteresis loop is partly inverted). A change in the nature of the hysteresis loop occurs after heat treatment at $T = 350$°C [50]. With a reduction in the diameter of the fibers to $d_f = 86$ μm, the inversion is retained in both the deformed and heat-treated states. The decrease in the fiber diameter to $d_f = 64$ μm leads to the disappearance of the inversion of the hysteresis loops of magnetic susceptibility; however, it manifests itself after heat treatment. With a further decrease in d_f (to 9 μm), no inversion of the hysteresis loops is observed.

Constricted hysteresis loops of magnetic susceptibility were observed in Fe–Ni–Co alloys (the *permin-var* effect) [59, 60], in magnesium–zinc ferrites with an impurity of cobalt oxide subjected to heat treatment [60], in nanocrystalline boron-containing magnetic

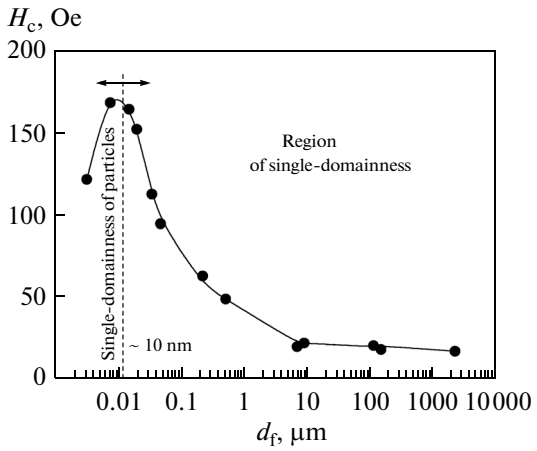

Fig. 4. Dependence of the coercive force H_c of Cu–Fe composites on the diameter of fibers.

materials based on iron and cobalt [61, 62], and also in the layered Ag/Ni [63] and CoO/Co [64] composites. In all these cases, the behavior of constricted hysteresis loops can be qualitatively explained within the framework of a two-phase model with two nonidentical phases, which are characterized by uniaxial magnetic anisotropy and antiferromagnetic interaction between them [62]. In armco iron used to produce Cu–Fe composites, the concentration of impurities is relatively small (~0.1 wt %) and the formation in it of regions that noticeably differ in composition is highly improbable. Nevertheless, as was shown by the methods of optical microscopy [51, 53], microindentation [50], and X-ray diffraction analysis, a solid solution of iron in copper that is characterized by the coercive force and magnetic permeability differing from those of the iron fibers can be formed in the composite. Deformation and annealing can change the relationships between these parameters, which leads to the changes observed in the nature of the hysteresis loops of low-frequency magnetic susceptibility [50].

3.3.4. Coercive force. With decreasing d_f, the coercive force H_c of fibrous Cu–Fe composites changes weakly up to $d_f \approx 10$ μm; then, it grows and reaches a maximum at a certain critical value $d_{cr} \approx 10$–15 nm, after which it decreases (Fig. 4) [53]. The obtained dependence of H_c on d_f is described adequately within the framework of the theory of the magnetization reversal of small ferromagnetic particles. An increase in H_c at 15 nm $< d_f <$ 10 μm is due to an increasing role of pinning of domain walls by the interphase boundaries, structural defects, and centers of elastic stresses caused by plastic deformation [65]. At $d_f <$ 15 nm, the thickness of domain walls becomes comparable with the grain size. The existence of domain walls becomes energetically unfavorable, and the crystallites become single-domain. The heat treatment at 550°C leads to a reduction in the coercive force by approximately a factor of 1.5, which is connected with an increase in the structural perfection of crystallites due to processes of recovery and recrystallization.

According to the theory of single-domain state developed by Kondorskii [66], the particle of a critical size possesses a maximum coercive force

$$H_{c\max} = 2K_{an}/M_s, \quad (1)$$

where K_{an} is the effective anisotropy constant and M_s is the saturation magnetization. This is caused by the fact that the change in magnetization occurs in this case via the coherent rotation of spins rather than by the motion of domain walls. At smaller diameters, the single-domain particle preserves its uniform magnetization. However, in this case, a decrease occurs in the anisotropy energy $E_{an} = K_{an}V$ (where V is the volume of the particle), and E_{an} becomes comparable with kT. The particle becomes similar to a paramagnetic atom with a large magnetic moment, and the transition into a superparamagnetic state occurs $(H_c \to 0)$ [67]. The beginning of this transition is observed in the experiment at $d_f < d_{cr}$ (Fig. 4).

The critical value $d_{cr} \approx 10$–15 nm obtained is in good agreement with the values given by other authors. For example, in granulated iron films, the value of d_{cr} found for room temperature was 15 nm [68]; in nanopowders, a value $d_{cr} \approx 22$–23 nm was obtained [69]; and, in [70], a value $d_{cr} \approx 25$ nm is given for small metallic particles. An insignificant spread of the values observed is most likely caused by the different shape of the particles and, correspondingly, by the different values of their demagnetizing factors. According to [66], d_{cr} is proportional to $N^{-1/2}$, where N is the demagnetizing factor of a single-domain ellipsoid along its short axis. The problem of the critical dimension for the single-domain state is discussed in a number of reviews [71, 72]. A theoretical estimation for the single-domain particles of a spherical shape gives a value $d_{cr} =$ 14 nm [73], which almost coincides with that obtained in this work.

3.3.5. Curie temperature. The Curie temperature T_C decreases monotonically from 745 to 715°C as the diameter of the fibers decreases from 160 μm to 3 nm, which is connected with changes in the exchange energy, anisotropy energy, and magnetoelastic energy [54]. Namely, an increase in the exchange energy favors the retention of a magnetic order and a shift of the Curie temperature into the region of higher temperatures. In turn, an increase in the anisotropy energy and in the magnetoelastic energy that occurs with a decrease in the size of fibers leads to a disordering of spins and to a decrease in T_C. Thus, the changes in T_C in the composites in question are determined by the competition of these two opposite tendencies with the predominance of the latter [74]. One additional reason for the change in T_C is possible, which is connected with an increase in the mutual dissolution of copper and iron at large deformations and small d_f [29]. As a

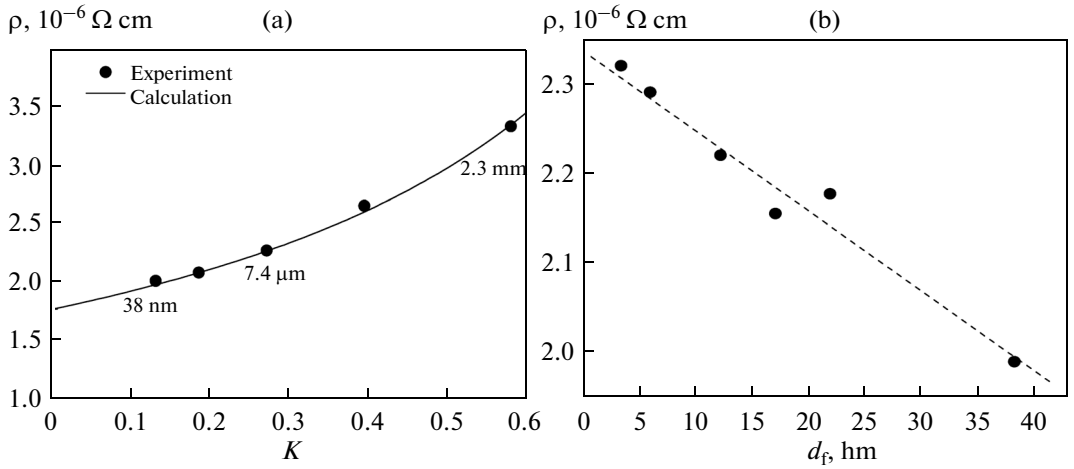

Fig. 5. Dependence of the resistivity of Cu–Fe composites on (a) the volume content of iron and (b) size of fibers.

result, at the interphase boundaries there appears a layer representing a solid solution of iron in copper. In this layer, naturally, the value of the exchange integral changes and, therefore, according to the Weiss molecular-field theory, the value of T_C also changes as follows:

$$T_C = 2zJS(S+1)/3k, \quad (2)$$

where z is the coordination number (for bcc iron, $z = 8$), J is the exchange integral, and S is the spin quantum number.

After the thermocycling of the composites at 20–900°C, the value of T_C grows, which is caused by an increase in grain size due to the process of recrystallization [54].

3.3.6. Resistive properties. It is known that, in fine-grained metals, in particular upon the transition into the region of nanosizes, the role of scattering of free charge carriers at the lattice defects and grain boundaries grows substantially [75–77]. This leads to an increase in the resistivity ρ. The dependence of ρ of the Cu–Fe composites on the volume content of iron in the range of the fiber sizes of 2.3–38 nm agrees well with that calculated according to the rule of mixtures in the case of the parallel connection of the copper and iron components of the composite (Fig. 5a) [51, 52]. With a further decrease in d_f, a deviation from the rule of mixtures is observed and ρ grows noticeably compared with the calculated value (Fig. 5b).

The increase in the electrical resistance upon the transition into the region of the nanometer values of d_f (Fig. 5b) is caused by the decrease in the sizes of structure elements. In nanostructured copper with the size of grains $d_g \approx 7$ nm, ρ grows by an order of magnitude compared with the coarse-grained copper and reaches 10–30 μΩ cm [77, 78]. In composites in question, no significant decrease in the size of copper grains occurs because of the application of repeated technological annealing upon the production of the composites. As a result, taking into account the fact that the resistance of iron fibers is shunted by the copper matrix, the observed increase in ρ is relatively small. The magnitude of the resistivity of Cu–Fe composites with nanometer fibers exceeds that of the pure recrystallized copper of grade M0b by only 13–25%.

Figure 6 demonstrates the strength/electrical-conductivity relationships for Cu–Fe composites obtained by different methods [4, 12–14, 16, 24, 51, 52]. It follows from this figure that the best combination of the electrical conductivity (80–90% IACS) and strength (900–1000 MPa) is achieved with the application of methods of powder metallurgy and SPD (packet HE). This effect is caused by the formation of a nanostructure in the composites and by the reduction in the

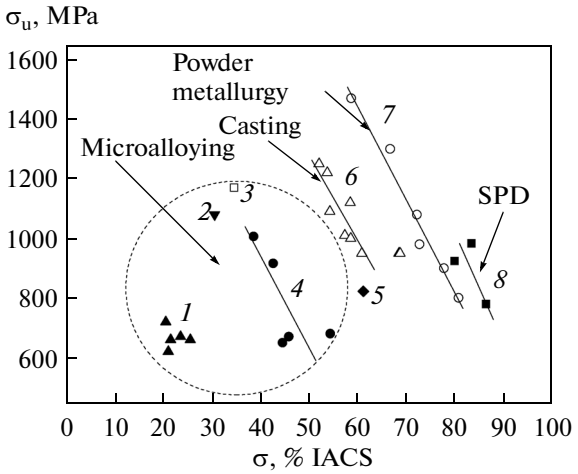

Fig. 6. Relationship between the ultimate strength and electrical conductivity for Cu–Fe composites obtained by the microalloying by (*1*) RE, (*2*) Al, (*3*) Mg, (*4*) Ag, (*5*) Zr, and by the methods of (*6*) casting, (*7*) powder metallurgy, and (*8*) SPD.

mutual solubility of copper and iron as a result of the use of reduced temperatures (20–500°C) in the above-described technological processes.

4. CONCLUSIONS

The Cu–Fe composites are functional materials that possess a unique combination of electrical, magnetic, and mechanical properties. The realization of these properties is feasible due to the wide possibilities of the methods of pressure treatment. Their application makes it possible to construct an optimum structure of the composites that consists of a heterogeneous system of strengthening fibers (layers) uniformly distributed in the conducting copper matrix.

Each of the methods of obtaining Cu–Fe composites considered above has advantages and disadvantages. Thus, the casting method makes it possible to form articles of a complex shape with low expenditures for production; powder metallurgy enables one to obtain soft-magnetic composites with excellent strength (up to 1500 MPa) and satisfactory electrical conductivity (60–70% IACS). The method of packet hydroextrusion is irreplaceable when preparing magnetically hard wire from the fibrous composite that is characterized by good strength (to 1000 MPa) and conducting (80–90% IACS) properties, precise geometric dimensions, and high surface finish. The selection of efficient technology for producing Cu–Fe composites is in first turn determined by their field of application as either soft magnetic or magnetically hard materials.

When producing Cu–Fe composites, one should note the following facts:

(1) the existence of the coercive force, which can be increased considerably (to 20 times) by decreasing the size of grains (fibers, layers);

(2) the formation of a solid solution of iron in copper, the amount of which increases with increasing temperature and degree of deformation, which in turn leads to the strengthening of the composites with a significant reduction in the electrical conductivity and coercive force.

Taking these factors into account makes it possible to obtain Cu–Fe composites with different combinations of magnetic, mechanical, and electrical properties by the variations in the parameters of the employed technological process (time, temperature, mode and regime of deformation) and the source material (material purity, size of powders).

REFERENCES

1. N. D. Stepanov, A. V. Kuznetsov, G. A. Salishchev, N. E. Khlebova, and V. I. Pantsyrny, "Evolution of microstructure and mechanical properties in Cu–14% Fe alloy during severe cold rolling," Mater. Sci. Eng., A **564**, 264–272 (2013).
2. B. I. Shapoval, V. M. Azhazha, V. M. Arzhavitin, I. B. Dolya, V. Ya. Sverdlov, M. A. Tikhonovskii, and V. G. Yarovoi, "Some physical and mechanical properties of Cu–Fe microcomposite," Vopr. At. Nauki Tekh., Ser.: Vakuum, Chistye Mater., Sverkhprovod., No. 1, 133–135 (2002).
3. W. Grünberger, M. Heilmaier, and L. Schultz, "High-strength, high-nitrogen stainless steel–copper composite wires for conductors in pulsed high-field magnets," Mater. Lett. **52**, 154–158 (2002).
4. J. D. Verhoeven, S. C. Chueh, and E. D. Gibson, "Strength and conductivity of in situ Cu–Fe alloys," J. Mater. Sci. **24**, 1748–1752 (1989).
5. Liang-Cai Maa, Jian-Min Zhang, and Ke-Wei Xu, "Magnetic and electronic properties of Fe/Cu multilayered nanowires: A first-principles investigation," Phys. E: Low-Dimen. Syst. Nanostruct. **50**, 1–5 (2013).
6. Yu. L. Zarapin, N. A. Chichenev, and N. G. Chernilevskaya, *Production of Composite Materials by Pressure Forming* (Metallurgiya, Moscow, 1991) [in Russian].
7. X. P. Lu, D. W. Yao, Y. Chen, L. T. Wang, A. P. Dong, L. Meng, and J. B. Liu, "Microstructure and hardness of Cu–12 wt. % Fe composite at different drawing strains," J. Zhejiang Univ. Sci. A. **5**, 149–156 (2014).
8. P. D. Funkenbusch and T. H. Courtney, "Microstructural strengthening in cold-worked in situ Cu–14.8 vol % Fe composites," Scr. Metall. **15**, 1349–1354 (1981).
9. C. Biselli and D. G. Morris, "Microstructure and strength of Cu–Fe in situ composites after very high drawing strains," Acta Mater. **44**, 493–504 (1996).
10. W. A. Spitzig, L. S. Chumbley, J. D. Verhoeven, Y. S. Go, and H. L. Downing, "Effect of temperature on the strength and conductivity of a deformation processed Cu–20% Fe composite," J. Mater. Sci. **27**, 2005–2011 (1992).
11. P. D. Funkenbusch and T. H. Courtney, "On the strength of heavily cold worked in situ composites," Acta Metall. **33**, 913–922 (1985).
12. H. Gao, J. Wang, D. Shu, and B. Sun, "Effect of Ag on the microstructure and properties of Cu–Fe in situ composites," Scr. Mater. **53**, 1105–1109 (2005).
13. Zhiwei Wu, Jindong Zhang, C. Yi, and Liang Meng, "Effect of rare earth addition on microstructural, mechanical and electrical characteristics of Cu–6% Fe microcomposites," J. Rare Earths **27**, 87–91 (2009).
14. Z. Yao, M. Ma, Q. Liu, and F. Zhao, "Influence of additional element Zr on strength and conductivity of fiber-reinforced Cu–Fe wire," Procedia Eng. **16**, 594–600 (2011).
15. B. Sun, H. Gao, J. Wang, and D. Shu, "Strength of deformation processed Cu–Fe–Ag in situ composites," Mater. Lett. **61**, 1002–1006 (2007).
16. J. S. Song, S. I. Hong, and Y. G. Park, "Deformation processing and strength/conductivity properties of Cu–Fe–Ag microcomposites," J. Alloys Compd. **388**, 69–74 (2005).
17. R. F. Bunshah, R. Nimmagadda, H. J. Doerr, B. A. Movchan, N. I. Grechanuk, and E. V. Dabizha, "Structure and property relationships in microlaminate

Ni–Cu and Fe–Cu condensates," Thin Solid Films **72**, 261–275 (1980).

18. O. F. Bakkaloğlu, "A magnetic study of sputtered Fe/Cu multilayer films," J. Magn. Magn. Mater. **182**, 324–328 (1998).
19. F. Petroff, A. Barthelemy, D. H. Mosca, D. K. Lottis, A. P. Fert, A. Schroeder, W. P. Pratt, Jr., R. Loloee, and S. Lequien, "Oscillatory interlayer exchange and magnetoresistance in Fe/Cu multilayers," Phys. Rev. B: Condens. Matter **44**, 5355–5357 (1991).
20. S. Pizzini, F. Baudelet, D. Chandesris, A. Fontaine, H. Magnan, J. M. George, F. Petroff, A. Barthelemy, A. Fert, R. Loloee, and P. A. Schroeder, "Structural characterization of Fe/Cu multilayers by X-ray absorption spectroscopy," Phys. Rev. B: Condens. Matter **46**, 1253–1256 (1992).
21. J. Xuesong, Xu. Huibin, and G. Shengkai, "The electrical conductivity characteristics of Fe/Cu nano-scale multilayer materials," Science in China (Ser. E) **44** (1), 83–88 (2001).
22. C. Bisellp and D. G. Morris, "Ìicrostructure and strength of Cu–Fe in situ composites obtained from prealloyed Cu–Fe powders," Acta Metall. Mater. **42**, 163–176 (1994).
23. Y. S. Go and W. A. Spitzig, "Strengthening in deformation-processed Cu–20% Fe composites," J. Mater. Sci. **26**, 163–171 (1991).
24. G. A. Jerman, I. E. Anderson, and J. D. Verhoeven, "Strength and electrical conductivity of deformation-processed Cu–15 vol % Fe alloys produced by powder metallurgy techniques," Metall. Trans. A **24**, 35–42 (1993).
25. J. Z. Jiang, C. Gente, and R. Bormann, "Mechanical alloying in the Fe–Cu system," Mater. Sci. Eng., A **242**, 268–277 (1998).
26. L. He and E. Ma, "Processing and microhardness of bulk Cu–Fe nanocomposites," Nanostruct. Mater. **7**, 327–339 (1996).
27. T. Ambrose, A. Gavrin, and C. L. Chien, "Magnetic properties of metastable fcc Fe–Cu alloys prepared by high energy ball milling," J. Magn. Magn. Mater. **124**, 15–19 (1993).
28. N. A. Azarenkov, V. M. Beresnev, A. D. Pogrebnyak, L. V. Malikov, and P. V. Turbin, *Nanomaterials, Nanocoatings, Nanotechnology* (KhNU im. V. N. Karazina, Kharkov, 2009) [in Russian].
29. X. Quelennec, A. Menand, J. M. le Breton, R. Pippan, and X. Sauvage, Homogeneous Cu–Fe supersaturated solid solutions prepared by severe plastic deformation," Philos. Mag. **90**, 1179–1195 (2010).
30. F. Matthews and R. D. Rawlings, *Composite Materials. Engineering and Science* (CRC Press, Boca Raton, Fla, 1999; Tekhnosfera, Moscow, 2003).
31. R. Z. Valiev and I. V. Aleksandrov, *Nanostructured Materials Obtained by Severe Plastic Deformation* (Logos, Moscow, 2000) [in Russian].
32. R. Z. Valiev and I. V. Aleksandrov, *Bulk Nanostructured Metallic Materials* (Akademkniga, Moscow, 2007) [in Russian].
33. Ya. E. Beigel'zimer, V. N. Varyukhin, D. V. Orlov, and S. G. Synkov, *Twist Extrusion—The Process for Strain Accumulation* (TEAN, Donetsk, 2003) [in Russian].
34. X. Sauvage, F. Wetscher, and P. Pareige, "Mechanical alloying of Cu and Fe induced by severe plastic deformation of a Cu–Fe composite," Acta Mater. **53**, 2127–2135 (2005).
35. Y. Saito, H. Utsunomiya, N. Tsuji, and T. Sakai, "Novel ultra-high straining process for bulk materials—Development of the accumulative roll-bonding (ARB) process," Acta Mater. **47**, 579–583 (1999).
36. I. M. Neklyudov, V. A. Belous, V. N. Voevodin, S. Yu. Didenko, N. I. Il'chenko, Yu. S. Didenko, Yu. N. Il'chenko, A. G. Rudenko, and G. N. Tolmacheva, "Mechanical properties and structure of microlaminates of copper–iron system," Vopr. At. Nauki Tekhn., Ser. Fiz. Radiat. Povrezhd. Radiat. Materialoved., No. 5, 95–101 (2010).
37. B. Huang, K. N. Ishihara, and P. H. Shingu, "Bulk nano-scale Fe/Cu multilayers produced by repeated pressing–rolling and their magnetoresistance," Mater. Sci. Lett. **19**, 1763–1765 (2000).
38. B. Huang, K. N. Ishihara, and P. H. Shingu, "Preparation of high strength bulk nano-scale Fe/Cu multilayers by repeated pressing–rolling," Mater. Sci. Lett. **20**, 1669–1670 (2001).
39. M. I. Karpov, B. A. Gnessin, V. I. Vnukov, N. V. Medved, V. P. Korjov, G. E. Abrosimova, and I. M. Khodoss, "The formation of the structure and mechanical properties of multi-layered metallic composites with nanometrical layers thickness," *Proc. 16th Int. Plansee-Semin.*, Reutte, Tirol, Austria. 2005, vol. 1, pp. 785–795.
40. M. I. Karpov, V. I. Vnukov, N. V. Medved', K. G. Volkov, and I. I. Khodos, "Multilayered Cu–Fe composite with nanometric thickness of layers," Materialovedenie, No. 1, 36–39 (2005).
41. V. P. Korzhov and M. I. Karpov, "Mechanical properties of multilayered micro- and nanocomposite materials from deformed metals obtained by diffusion welding and rolling methods," *Proc. Int. Sci.-Tech. Conf. "Contemporary Methods and Technologies of Material Formation and Treatment"* Minsk, 2010, in 3 books. Book 1, pp. 123–128 [in Russian].
42. M. I. Karpov, V. P. Korzhov, V. N. Zverev, V. I. Vnukov, and I. S. Zheltyakova, "Microstructure and critical density of film composite current with nanosized layers from Nb–Ti superconducting layers," Fiz. Tekh. Vys. Davl. **18** (4), 70–76 (2008).
43. O. B. Dugadko, M. Matrosov, V. Z. Spuskanyuk, B. A. Shevchenko, and E. O. Medveds'ka, UA Patent 56651 (2003).
44. V. N. Varyukhin, A. B. Dugadko, N. I. Matrosov, V. Z. Spuskanyuk, L. F. Sennikova, E. A. Pavlovskaya, B. A. Shevchenko, and O. N. Mironova, "Regularities of strengthening of fiber materials obtained by packet hydroextrusion," Fiz. Tekh. Vys. Davl. **13** (1), 96–105 (2003).
45. S. G. Synkov, V. G. Synkov, and A. N. Sapronov, "Packet hydroextrusion of microfibers from chromium–nickel steels," Fiz. Tekh. Vys. Davl. **6** (2), 141–145 (1996).
46. F. Wacquant and S. Denolly, "Hexagonal array of submicroscopic ferromagnetic wires obtained by multiple

extrusion of bulk samples," J. Appl. Phys. **85**, 5483–5485 (1999).

47. S. Gangopadhyay, G. C. Hadjipanayi, B. Dale, C. M. Sorensen, and K. J. Klabunde, "Magnetism of ultrafine particles," Nanostruct. Mater. **1**, 77–81 (1992).
48. I. V. Zolotukhin, "Nanocrystalline metallic materials," Soros. Obraz. Zh., No. 1, 103–106 (1998).
49. G. I. Frolov, O. I. Bachina, M. M. Zav'yalova, and S. I. Ravochkin, "Magnetic properties of nanoparticles of 3*d* metals," Tech. Phys. **53**, 1059–1064 (2008).
50. A. N. Cherkasov, V. A. Beloshenko, V. Z. Spuskanyuk, V. Yu. Dmitrenko, and B. A. Shevchenko, "Low-frequency magnetic susceptibility of fiber Fe–Cu composites," Phys. Met. Metallogr. **104**, 136–141 (2007).
51. V. A. Beloshenko, V. N. Varyukhin, V. Yu. Dmitrenko, Yu. I. Nepochatykh, and A. N. Cherkasov, "Cu–Fe fiber composites obtained by packet hydroextrusion method: Structure, mechanical and resistive properties," Fiz. Tekh. Vys. Davl. **20**, 110–118 (2010).
52. V. A. Beloshenko, V. Yu. Dmitrenko, and V. V. Chishko, "Properties of metallic fiber composites with copper matrix obtained by packet hydroextrusion method," Obrab. Mater. Davleniem, No. 1, 85–89 (2012).
53. V. A. Beloshenko, V. N. Varyukhin, V. Yu. Dmitrenko, Yu. I. Nepochatykh, V. Z. Spuskanyuk, A. N. Cherkasov, and B. A. Shevchenko, "Structure and magnetic properties of Cu–Fe fiber composites obtained using packet hydrostatic extrusion," Tech. Phys. **54**, 1790–1794 (2009).
54. V. A. Beloshenko, V. N. Varyukhin, V. Yu. Dmitrenko, Yu. I. Nepochatykh, and A. N. Cherkasov, "Curie temperature of Cu–Fe fiber composites obtained by packet hydroextrusion," Vopr. Materialoved. **66** (2), 37–41 (2011).
55. N. Yu. Zolotorevskii, E. V. Nesterova, V. V. Rybin, and Yu. F. Titovets, "Micro- and macrotexture evolution during steel-wire drawing," Phys. Met. Metallogr. **99**, 73–79 (2005).
56. G. Mazzone and M. V. Antisari, "Structural and magnetic properties of metastable fcc Cu–Fe alloys," Phys. Rev. B: Condens. Matter **54**, 441–446 (1996).
57. A. R. Yavari, P. J. Desré, and T. Benameur, "Mechanically driven alloying of immiscible elements," Phys. Rev. Lett. **68**, 2235–2238 (1992).
58. V. M. Beresnev, A. D. Pogrebnyak, N. A. Azarenkov, V. I. Farenik, G. V. Kirik, "Nanocrystalline and nanocomposite coatings, structure, properties," Phys. Surf. Eng. **5**, 4–27 (2007).
59. R. Bozort, *Ferromagnetism* (Van Nostrand, 1951; Inostrannaya Literatura, Moscow, 1956).
60. L. I. Rabkin, *High-Frequency Ferromagnets* (Fizmatgiz, Moscow, 1960) [in Russian].
61. N. I. Noskova, V. V. Shulika, A. G. Lavrent'ev, A. P. Potapov, and G. S. Korzunin, "Effect of nanocrystallization conditions on the structure and magnetic properties of Fe- and Co-based amorphous alloys," Phys. Met. Metallogr. **100**, 557–563 (2005).
62. E. E. Shalygina, I. Skorvanek, P. Svek, V. A. Mel'nikov, and N. M. Abrosimova, "Inverted near-surface hysteresis loops in heterogeneous (nanocrystalline/amorphous) $Fe_{81}Nb_7B_{12}$ alloys," J. Exper. Theor. Phys. **99**, 544–551 (2004).
63. C. A. dos Santos and B. Rodmacq, "Inverted and crossed hysteresis loops in Ag/Ni multilayers," J. Magn. Magn. Mater. **147**, L250–L252 (1995).
64. M. J. O'Shea and A. Al-Sharif, "Inverted hysteresis in magnetic systems with interface exchange," J. Appl. Phys. **7**, 6673–6675 (1994).
65. *Physical Metallurgy*, Ed. by R. W. Cahn and P. Haasen (North-Holland, New York, 1983; Metallurgiya, Moscow, 1987).
66. E. I. Kondorskii, "Nature of high coercive force of low-dispersed ferromagnets and the theory of single-domain structure," Izv. Akad. Nauk SSSR, Ser. Fiz. **16**, 398–411 (1952).
67. Belov, K.P., *Magnetostriction Phenomena and Their Applications* (Nauka, Moscow, 1987) [in Russian].
68. C. Chen, O. Kitakami, and Y. Shimoda, "Particle size effects and surface anisotropy in Fe-based granular films," J. Appl. Phys. **84**, 2184–2188 (1998).
69. E. F. Kneller and F. E. Luborsky, "Particle size dependence of coercivity and remanence of single–domain particles," J. Appl. Phys. **34**, 656–658 (1963).
70. S. A. Nepiiko, *Physical Properties of Small Metallic Particles* (Naukova Dumka, Kiev, 1985) [in Russian].
71. W. F. Brown, *Micromagnetics* (Wiley, New York, 1963).
72. E. F. Kneller, *Magnetism and Metallurgy* (Academc, New York, 1969), Vol. 1.
73. P. A. Chernavskii, "The new in magnetic methods of metal-coated catalyst study," Ross. Khim. Zh. **46** (3), 19–30 (2002).
74. T. I. Arbuzova, B. A. Gizhevskii, R. G. Zakharov, S. A. Petrova, and N. M. Chebotaev, "Magnetic susceptibility of nanostructural manganite $LaMnO_{3+\delta}$ produced by mechanochemistry method," Phys. Solid State **50**, 1487–1494 (2008).
75. R. A. Andrievskii and A. M. Glezer, "Size effects in nanocrystalline materials: I. Structure characteristics, thermodynamics, phase equilibria, and transport phenomena," Phys. Met. Metallogr. **88**, 48–66 (1999).
76. R. A. Andrievskii and A. M. Glezer, "Size effects in nanocrystalline materials: II. Mechanical and physical properties," Phys. Met. Metallogr. **89**, 83–103 (2000).
77. A. I. Gusev, "Effects of the nanocrystalline state in solids," Phys–Usp. **41**, 49–76 (1998).
78. V. A. Pozdnyakov, "Mechanisms of plastic deformation and the anomalies of the Hall–Petch dependence in metallic nanocrystalline materials," Phys. Met. Metallogr. **96**, 105–118 (2003).

Translated by S. Gorin